REDCRAFT: A Computational Platform Using Residual Dipolar Coupling NMR Data for Determining Structures of Perdeuterated Proteins Without NOEs

Casey A. Cole[1], Nourhan S. Daigham[2], Gaohua Liu[2,3],
Gaetano T. Montelione[4], Homayoun Valafar[1,*]

[1] Department of Computer Science & Engineering, University of South Carolina, Columbia, South Carolina 29208, USA.
[2] Center for Advanced Biotechnology and Medicine, and Department of Molecular Biology and Biochemistry, Rutgers, The State University of New Jersey, Piscataway, NJ 08854, USA.
[3] Nexomics Biosciences, 5 Crescent Ave, Rocky Hill, NJ 08553, USA
[4] Department of Chemistry and Chemical Biology, and Center for Biotechnology and Interdisciplinary Studies, Rensselaer Polytechnic Institute, 110 Eighth Street, Troy, NY, 12180, USA
[5] Department of Biochemistry and Molecular Biology, The Robert Wood Johnson Medical School, Rutgers, The State University of New Jersey, Piscataway, NJ 08854, USA.

Conflict of Interest Statement: G.L. is Chief Scientific Officer at Nexomics. Biosciences, Inc. G.T.M. is Scientific Founder of Nexomics Biosciences, Inc. These affiliations are disclosed for information purposes, and do not imply any bias in the collection or interpretation of the data presented here.

Abstract:

Nuclear Magnetic Resonance (NMR) spectroscopy is one of the two primary experimental means of characterizing macromolecular structures, including protein structures. Structure determination by NMR spectroscopy has traditionally relied heavily on distance restraints derived from nuclear Overhauser effect (NOE) measurements. While structure determination of proteins from NOE-based restraints is well understood and broadly used, structure determination by NOEs imposes increasing quantity of data for analysis, increased cost of structure determination and is less available in the study of perdeuterated proteins. In the recent decade, Residual Dipolar Couplings (RDCs) have been investigated as an alternative source of data for structural elucidation of proteins by NMR. Several methods have been reported that utilize RDCs in addition to NOEs, and a few utilize RDC data alone. While these methods have individually demonstrated some successes, none of these methods have exposed the full potential of protein structure determination from RDCs. To date, structure determination of proteins from RDCs is limited to small proteins (less than 8.5 kDa) using RDC data from many alignment media (>3) that cannot be collected from larger proteins. Here we present the latest version of the REDCRAFT software package designed for structure determination of proteins from RDC data alone. We have demonstrated the success of REDCRAFT in structure determination of proteins ranging in size from 50 to 145 residues using experimentally collected data and large proteins (145 to 573 residues) using simulated RDC data that can be collected from perdeuterated proteins. Finally, we demonstrate the accuracy of structure determination of REDCRAFT from RDCs alone in application to the structurally novel PF.2048 protein. The RDC-based structure of PF.2048 exhibited 1.0 Å of BB-RMSD with respect to the NOE-based structure by only using a small amount of backbone RDCs (~3 restraints per residue)

compared to what is required by other approaches.

Author Summary:

Residual Dipolar Couplings have the potential to reduce the cost and the time needed to characterize protein structures. In addition, RDC data have been demonstrated to concurrently elucidate structure of proteins, perform assignment of resonances, and be used in characterization of the internal dynamics of proteins. Given all the advantages associated with the study of proteins from RDC data, based on the statistics provided by the Protein Databank (PDB), surprisingly the only 124 proteins (out of nearly 150,000 proteins) have utilized RDCs as part of their structure determination. Even a smaller subset of these proteins (approximately 7) have utilized RDCs as the primary source of data for structure determination. The impeding factor in the use of RDCs is the challenging computational and analytical aspects of this source of data. In this report, we demonstrate the success of the REDCRAFT software package in structure determination of proteins using RDC data that can be collected from small and large proteins in a routine fashion. REDCRAFT accomplishes the challenging task of structure determination from RDCs by introducing a unique search and optimization technique that is both robust and computationally tractable. Structure determination from routinely collectable RDC data using REDCRAFT can lead to faster and cheaper study of larger and more complex proteins by NMR spectroscopy in solution state.

Introduction

Nuclear Magnetic Resonance Spectroscopy is a well-recognized and utilized approach to structure determination of macromolecules including proteins. NMR spectroscopy has contributed to structural characterization of nearly 11,649 proteins based on statistics reported by the Protein DataBank(1-3) (PDB). Although NMR studies may in general be more time consuming and costly than X-ray crystallography, they provide the unique benefit of observing macromolecules in their native aqueous state, which provide a better understanding of molecular interactions and internal dynamics at various timescales and resolutions.

Despite the changes that NMR spectroscopy has observed over the years, the methodology in analysis of NMR data has made relatively little progress. Nearly all methods of NMR data analysis rely on a combination of Simulated Annealing(4, 5), Gradient Descent(4, 5), and Monte Carlo sampling(4, 5) to guide their protein structure calculations in satisfying the experimental constraints. The traditional approaches to characterization of protein structures by NMR spectroscopy have relied heavily on sidechain-sidechain based distance constraints(6), which are limited to a range of 2.5-5Å. The distance constraints obtained by NMR spectroscopy are often augmented with other heterogenous data such as backbone-backbone contacts, scalar couplings, and dihedral restraints. The structure of the target protein is then computed by deploying a combination of constrained Monte Carlo and Gradient Descent optimization routines. This combination of heterogeneous data and optimization techniques with well documented limitations(4, 7) has resulted in an inflated requirement for experimental data. The functional consequence of this mechanism of protein structure determination has manifested itself as inflated data acquisition time and the cost of structure determination, while also functionally limiting the upper boundary in the size of the proteins that can be studied by NMR spectroscopy.

In the recent years, Redisual Dipolar Couplings (RDC) has been recognized as a promising alternative to the traditional Nuclear Overhauser Effect (NOE) constraints. RDCs have distinct advantages over the traditional distance constraints(8-14). Generally, RDC data are more precise, easier to measure, and are capable of providing informative structural and dynamic information. Structure determination based primarily on RDC data requires new approaches that operate in fundamentally different ways from those that use NOE data. This is the primary reason that the legacy programs such as Xplor-NIH(15), CNS(16) or CYANA(17) are not appropriate for de novo structure determination purely by RDC data. Other contemporary methods have been presented(8, 13, 18-25) with a direct focus on characterization of structure from RDC data. While these programs address some of the shortcomings of the traditional approaches, their continued use of the conventional optimization techniques prevent full utilization of the rich information content of the RDC data. Some of these algorithms exhibit a direct or indirect reliance on completeness of the PDB and a thorough sampling of the protein fold-space(23, 24). Others utilize impractical number of RDCs(25-28) (e.g. 4 RDCs per residue collected in 5 alignment media) that cannot be routinely collected, especially on larger and perdeuterated proteins. Furthermore, all the existing RDC-based structure determination approaches deploy search strategies that continue to rely on the traditional optimization techniques such as Levenberg-Marquardt(29) or gradient descent. These approaches work for meticulously clean and complete datasets and therefore lack the needed practical robustness for the analysis of noisy or missing data. Finally, there is no currently existing software that is capable of concurrent structure determination and identification of internal motion in proteins. REDCRAFT illustrates a number of unique advantages, with its most unique feature consisting of a novel search methodology optimally suited for the analysis of RDC data.

Here we demonstrate the extended abilities of REDCRAFT in structure calculation of

proteins from Residual Dipolar Couplings (RDCs) that can be collected routinely from small and large proteins. More specifically, we demonstrate the feasibility of structure determination of proteins using only RDCs that can be obtained from perdeuterated proteins, namely backbone {C'-N, N-H^N, C'-H} in two alignment media. When available, our investigations are based on previously reported experimental RDC data, and when needed, the experimental data are augmented with synthetic data. We have demonstrated successful structure determination by REDCRAFT on eight proteins with a size range of 50 to 573 amino acids. Finally, REDCRAFT has been tested in structure determination of a novel protein, PF2048.1, and the results were validated in comparison to NOE based structures.

Results

In the following sections we present three sets of results, all of which demonstrate structure determination of proteins from RDCs alone to reduce the overall cost of structure determination. In the first set, we explored the structure determination of all proteins by REDCRAFT, for which sufficient experimental RDC data were deposited into the BMRB database. In each of these exercises, we used substantially smaller set of RDC data than the previously reported studies. In the second set of results, we have investigated the success of REDCRAFT in structure determination of large proteins using synthetically generated RDCs. The structure of these proteins had been previously characterized by distance constraints while including a very small subset of RDCs, therefore establishing the plausibility of RDC collection for these proteins. In the third exercise, we have characterized the structure of the novel protein PF2048.1 by the traditional NOE data and RDC data separately. Using the two structures, we established the accuracy of the RDC based structure from REDCRAFT to the conventional NOE based structure with using only a

fraction of the data.

Protein Structure Calculation Using Experimental RDCs

Table 1 and Figure 1 summarize the results of REDCRAFT structure calculation of proteins using only experimental RDC data. The listed five proteins in this table have been previously studied by NMR spectroscopy, for which enough experimental RDCs have been deposited to BMRB(30). In some instances, RDC data are missing for a large portion of a protein. In such instance, REDCRAFT accommodates fragmented structure determination and therefore the structural comparison to the target structure is reported as a range of BB-RMSD's calculated for each fragment. The fourth and fifth columns of Table 1 provide a quality of structural fitness to the RDC data as a Q-factor(31). In summary, a Q-factor over the threshold of 0.3 is considered a poorly fit structure, while values less than 0.2 are considered acceptable, and values less than 0.1 are considered exceptionally well-fit structures. The last column of Table 1 indicates the percentage of the data that was utilized by REDCRAFT compared to the number of constraints used previously. In general, as seen in Table 1, the obtained structures were less than 2Å from the target structures with sufficiently low Q-factors (indicating a reliable structure), while reducing the total data requirement by as much as 90%. In the following paragraphs, additional detailed results for each protein are discussed.

GB1 – The previously calculated NMR structure of GB1 (2PLP) was determined using 769 RDC restraints that included {N-H^N, N-C', C_α-C', H-C_α, H-C', C_α-C_β}, 127 long range H^N-H^N RDCs, and 54 Residual Chemical Shift (RCS) restraints from two alignment media(28). In this study, 209 RDC restraints (compared to the total of 950 restraints) were used to obtain a structure less than 1.5Å from both the X-Ray and NMR structures.

GB3 – For GB3, the dataset included the following RDCs from: {N-C', N-H^N, C_α-H_α, C_α-

161 C'} in five alignment media. Two previous studies used this full set of RDC data to determine a
162 structure of GB3 to within 1Å of the corresponding X-ray structure(32, 33). In a previous
163 REDCRAFT study(34), the structure of GB3 was determined using {N-H^N, C_α-H_α} RDCs in two
164 alignment media. However, the collection of {C_α-H_α} RDCs is uncommon due to sample
165 preparation requirement and added complexity in NMR data interpretation. Using these RDCs,
166 REDCRAFT was able to reconstruct the structure to within 0.6-2.4Å of the NMR structure. For
167 the purposes of this study, the RDC data was reduced to the vectors {N-C', N-H^N} since they can
168 be collected from perdeuterated protein samples. Utilization of these RDCs are more challenging
169 than the previous set due to their planarity with one another. Using these vectors, we were able to
170 calculate a structure of this protein with BB-RMSD of less than 2.5Å.

171 *Rubredoxin* – Previously, the structure of Rubredoxin was characterized to within 1.81Å
172 of the X-ray structure using the following RDC vectors: {N-C', N-H^N, C'-H, C_α-H_α, H^N-H_α, H_α-
173 H^N} in two alignment media(10). Again, to simulate an RDC set that could be collected from a
174 perdeuterated protein, that experimental RDC set was reduced to {N-H^N, C'-H} from two
175 alignment media. A BB-RMSD of 1.12Å and 1.02Å were obtained in relation to the NMR and X-
176 ray structures.

177 *ChR145* – As part of the original study of ChR145, {N-H^N, C'-N} RDCs were collected in
178 two alignment media (PEG and Phage) and an additional set of {N-H^N} RDCs were collected in a
179 third alignment medium (PAG). All RDCs were deposited into the SPINE(35) database. Utilizing
180 only these RDC restraints, REDCRAFT was able to produce structures with BB-RMSDs in the
181 range of 1.4Å -2.3Å. This is then compared to the traditional NMR structure that utilized 2,676
182 NOEs, 256 dihedral restraints and the 328 RDC restraints.

183 *SR10* – The structure of SR10 was obtained by NMR spectroscopy to within 2.0-2.5Å with

respect to an X-ray structure. The RDCs available for this protein were 3 sets of {N-H^N} RDCs. A fragmented study was utilized in this case due to large gaps in the RDC data. The original NOE-based structure utilized 1765 restraints (a mix of RDCs and NOEs) whereas our method only used 320 RDC data.

Table 1. Results for structure calculation using experimental RDCs is summarized.

Target Name	# Res.	BB-RMSD to NMR Structure (Å)	BB-RMSD to X-Ray Structure (Å)	Q Factor of Prev. Solved Structure	Q Factor of REDCRAFT Structure	% of Used Data
GB1	54	1.189	1.481	0.15, 0.11	0.098, 0.12	22%
GB3	54	1.9 - 2.5	1.3 - 2.2	0.034, 0.045	0.01 - 0.02, 0.02-0.34	23%
Rubredoxin	50	1.121	1.02	0.08, 0.52	0.33, 0.19	41%
ChR145	145	1.4 - 2.3	N/A	0.17, 0.18, 0.24	0.01 - 0.046, 0.01 - 0.038, 0.01 - 0.026	11%
SR10	145	1.1 - 2.4	1.6-2.4	0.9, 0.68, 0.89	0.028 - 0.05, 0.05 - 0.16, 0.06 - 0.32	18%

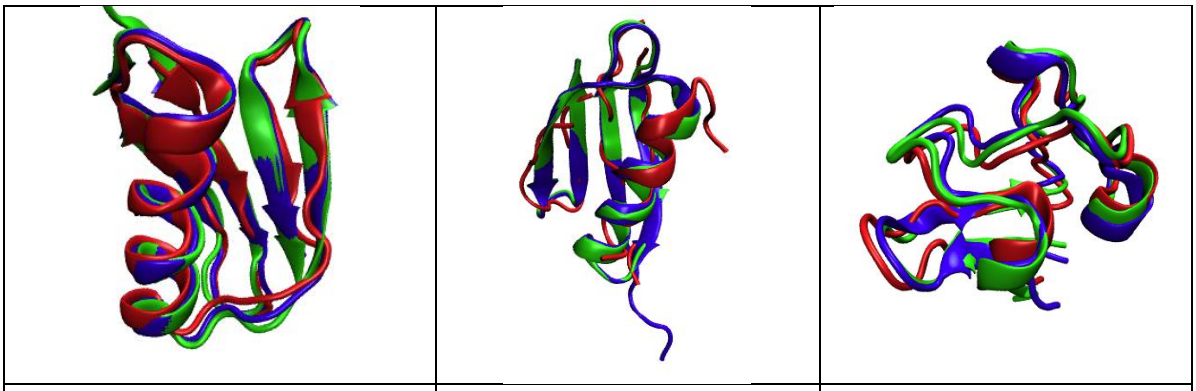

A **B** **C**

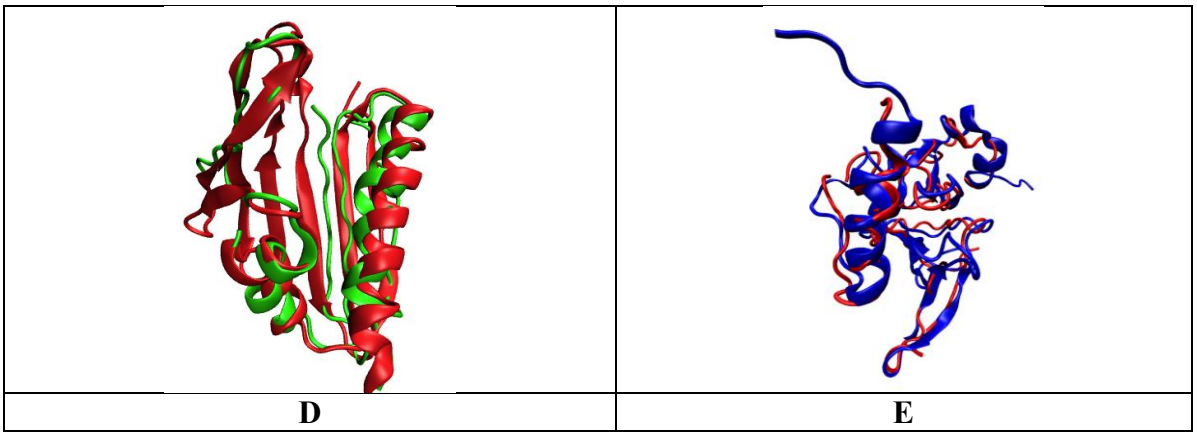

Figure 1. Results of REDCRAFT structure calculation (in red) compared to X-Ray structures (in blue) and, where applicable, traditional NMR Structures (in green) for A) GB1, B) GB3, C) Rubredoxin, D) ChR145, E) SR10.

Conventional and REDCRAFT Based Structure Determination of PF2048.1

Following the procedures outlined in the Materials and Methods section, two structures were characterized and deposited in the Protein Data Bank(36): one structure that did not include any RDC data that used a total of 2,574 total restricting restraints (PDB_id 6E4J, BMRB_id 30494), and one structure that included RDC (2,534 restricting restraints) (PDB_id 6NS8 and the same BMRB_id 30494). Comparison of these two structures demonstrates the impact of RDC during the last stages of structural refinement following the conventional methods of structure determiantion. Structure quality assessment metrics for these two NMR structures are presented in Supplementary Table S1. Overall, both structures (with and without RDCs) exhibited high quality structures, with excellent structure quality scores. The RDC Q-factors for the two alignment media M1 and M3 are 0.340 ± 0.020 and 0.320 ± 0.031, respectively for the models generated without RDCs, and 0.275 ± 0.015 and 0.280 ± 0.028, respectively, for models generated using RDC data as restraints. The DP scores, assessing how well the models fit to the unassigned NOESY peak list data, are 0.905 and 0.905 for the structures modeled without and with, respectively, RDC data. Molprobity packing scores(37), Richardson backbone dihedral angle analysis(38), and ProCheck(39) backbone and sidechain dihedral angle quality scores for well-defined regions of

these models, are also excellent. The backbone RMSD between the medoid models of the ensembles generated with and without RDC data is 0.745 Å. Taken together, this structure quality analysis demonstrates that the experimental NMR structures determined using the conventional approaches are excellent quality, and good reference states for assessing modeling methods using RDC data alone.

The structure of PF2048.1 was determined with only 228 RDCs that consisted of the backbone {C'-H, N-H^N, C'-N} vectors from the first alignment medium and backbone {N-H} from the second alignment medium. The final REDCRAFT structure exhibited 2.3Å of structural deviation from the target NOE structure before any structural refinement. This structure was then subjected to 20,000 rounds of Powell minimization in Xplor-NIH software package using the same 228 RDC restraints in order to resolve some minor Van Der Waal collisions. The Q-factors before and after minimization for both alignment media are shown in Table 2. It was shown that the Q-factor for M2 was slightly improved. Note that the Q-factor for M1 incurred a slight increase during minimization due to the correction of a Van der Waal collisions in the computed structure. Figure 2 illustrates superimposition of the REDCRAFT computed structure of PF2048.1 (in red) before and after minimization and the NOE structure without RDCs (in blue) and the NOE structure with RDCs (in yellow). The final structure exhibited Q-factors of 0.09 and 0.13 in the two alignment media respectively and a BB-RMSD of less than 1.0 Å with respect to both NOE structures (structures determined with and without RDCs).

Table 2. Results from structure calculation of PF2048.1 using 228 RDCs and secondary structure restraints are shown.

	Q factor M1	Q factor M2	BB-RMSD to NOE structure w/o RDCs (Å)	BB-RMSD to NOE structure w/ RDCs (Å)

Before refinement	0.041	0.158	2.38	2.24
After refinement	0.095	0.133	0.98	0.94

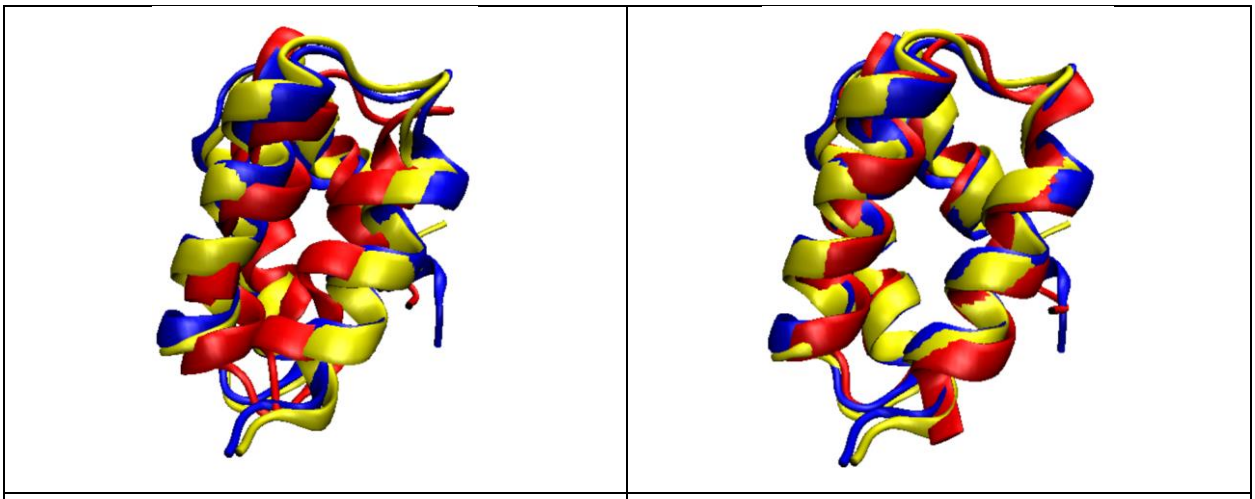

A **B**

Figure 2. Results for PF2048.1 (in red) A) before minimization and B) after minimization are shown superimposed to the NMR structure without RDCs (in blue) and the NMR structure with RDCs (in yellow).

Structure Calculation of Large Proteins

The results of structure calculation for large proteins using synthetic RDCs are shown in Table 3 and Figure 3. Although the structure of ChR145 was characterized by REDCRAFT using experimental data (reported in Table 1), here we have repeated the structure determination of this protein with synthetic data to illustrate the possibility of full structure determination (instead of a fragmented study) if adequate RDCs were collected. In this study, ChR145 was characterized in one full continuous segment with a BB-RMSD of 1.45Å with respect to the reference structure. In addition, the resulting structure had excellent Q-factors.

In the cases of Lpg1496 and Enzyme 1, fragmented study was performed due to contribution of structural noise discussed in the Materials and Methods section. For instance, in several cases, a single residue's dihedral angles were in severe violation of the Ramachandran space. In such instances, the structure determination was augmented with short refinement of each fragment followed by their integration using Xplor-NIH. For Lpg1496, the largest contiguous

fragment characterized as 138 residues in length displaying a BB-RMSD of 1.73Å. Additional fragments ranged from 50 to 75 residues in length. All fragments reported Q-factors indicative of reliable structure in each alignment medium as well as low BB-RMSDs to the reference structure. The longest fragment for Enzyme 1 was 208 residues, which exhibited a BB-RMSD of 1.78Å. All other fragments ranged from 50 to 100 residues in length. For the fragmented studies, all fragments were aligned to their respective structures and an average BB-RMSD was calculated (shown in the table).

Table 3. Results for structure calculation using synthetic RDCs is summarized.

Target Name	Reference Structure	# Res.	BB-RMSD to Reference Structure (Å)	Q Factor of REDCRAFT Structure in M1, M2
ChR145	2LEQ	145	1.45	0.057, 0.051
Lpg1496	5T8C	294	2.22	0.087, 0.068
Enzyme 1 from E. *coli*	2KX9	573	1.90	0.09, 0.07

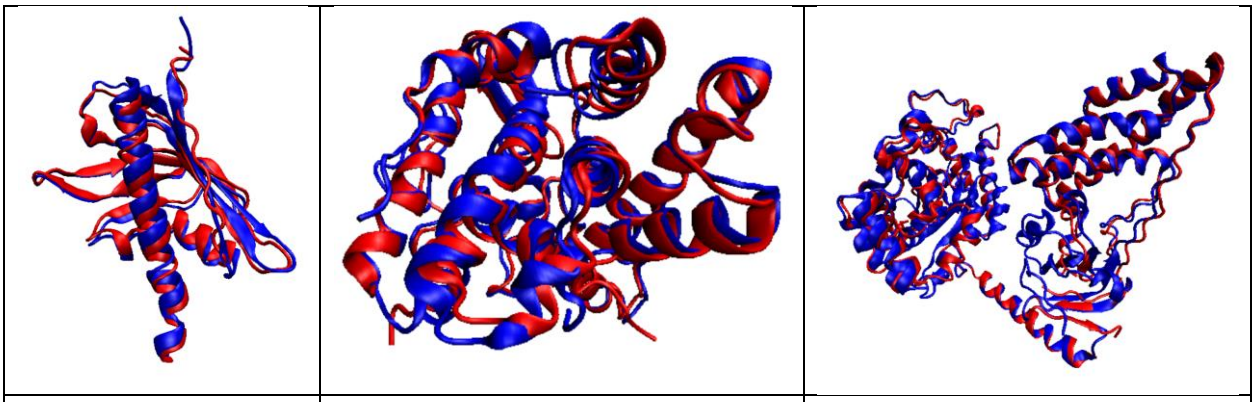

Figure 3. Results of REDCRAFT structure calculation (in red) compared to the reference structure (in blue) A) ChR145, B) Lpg1496 and C) Enzyme 1 from E. *coli*.

Discussion

Structure calculation of large proteins from RDCs using REDCRAFT is possible and can have numerous advantages. In this study, we have demonstrated the feasibility of calculating the

structure of proteins of varying sizes (50-573 amino acids) from RDCs using REDCRAFT. In addition, due to the novel search mechanism of REDCRAFT, we have demonstrated reliable folding of proteins with as little as 11% of the previously used data. Furthermore, we have shown that RDCs collected on perdeuterated proteins are sufficient for folding large proteins (as large as 573) with high accuracy. This is a significant achievement since in most cases, large proteins must be perdeuterated to be amenable for study by NMR spectroscopy. Using simulated RDCs, we also demonstrated that determination of large proteins is in fact possible using the minimal set of RDCs that can be acquired using perdeuterated samples. Lastly, we show REDCRAFT's ability to characterize an unknown protein with very little sequence or structural similarity to other proteins.

Structural elucidation of proteins from RDCs using REDCRAFT has other pragmatic advantages. For instance, characterization of protein structure does not have to be restricted to the entire protein. RECRAFT's approach allows for structural investigation of a fragment of the protein as demonstrated with proteins GB3, ChR145, and SR10. Isolated study of a targeted fragment of a protein will reduce the cost of structure determination and allow for study of larger proteins in a partitioned fashion. Furthermore, the combination of RDCs when analyzed with REDCRAFT, enables concurrent study of structure and dynamics of a protein as presented previously(34, 40, 41), also reducing the cost of such studies.

Methods

Residual Dipolar Couplings

Residual Dipolar Couplings (RDCs), an alternate source of data obtainable by NMR spectroscopy, had been observed as early as 1963 in pneumatic solutions(42). The recent reintroduction of RDCs due to the development of alignment media has presented this source of

data as a possible substitute to the conventional approach to structure determination by NMR spectroscopy. RDCs have been shown to be valuable for structural characterization of aqueous proteins(10, 12, 43, 44) and challenging proteins(40, 45-49), while enabling simultaneous study of structure and dynamics of proteins(9, 27, 40, 45, 50-53). Because RDCs can be used to characterize the structure of proteins with far less data than the traditional approaches, it presents a viable and cost-effective method of protein structure elucidation.

RDCs arise from the interaction of two magnetically active nuclei in the presence of the external magnetic field of an NMR instrument(54-57). This interaction is normally reduced to zero, due to the isotropic tumbling of molecules in their aqueous environment. The introduction of partial order to the molecular alignment reintroduces dipolar interactions by minutely limiting isotropic tumbling. This partial order can be introduced in numerous ways(58), including inherent magnetic anisotropy susceptibility of molecules(59), incorporation of artificial tags (such as lanthanides) that exhibit magnetic anisotropy(54), or in a liquid crystal aqueous solution(58) as illustrated in Figure 4. The RDC interaction phenomenon has been formulated in different ways(57, 60). In order to harness the computational synergy of RDC data, we utilize the matrix formulation of this interaction as shown in Eq (1). The entity S shown in Eq (1) and (2) represents the Saupe order tensor matrix(42, 54, 61) (the 'order tensor') that can be described as a 3x3 symmetric and traceless matrix. D_{max} in Eq (1) is a nucleus-specific collection of constants, r_{ij} is the separation distance between the two interacting nuclei (in units of Å), and v_{ij} is the corresponding normalized internuclear vector

$$D_{ij} = \left(\frac{D_{max}}{r_{ij}^3}\right) v_{ij} * S * v_{ij}^T \qquad \textit{Eq (1)}$$

$$S = \begin{bmatrix} S_{xx} & S_{xy} & S_{xz} \\ S_{xy} & S_{yy} & S_{yz} \\ S_{xz} & S_{yz} & S_{zz} \end{bmatrix} \qquad \textit{Eq (2)}$$

$$v_{ij} = \begin{pmatrix} cos\ (\theta_x) \\ cos\ (\theta_y) \\ cos\ (\theta_z) \end{pmatrix} \qquad \textit{Eq (3)}$$

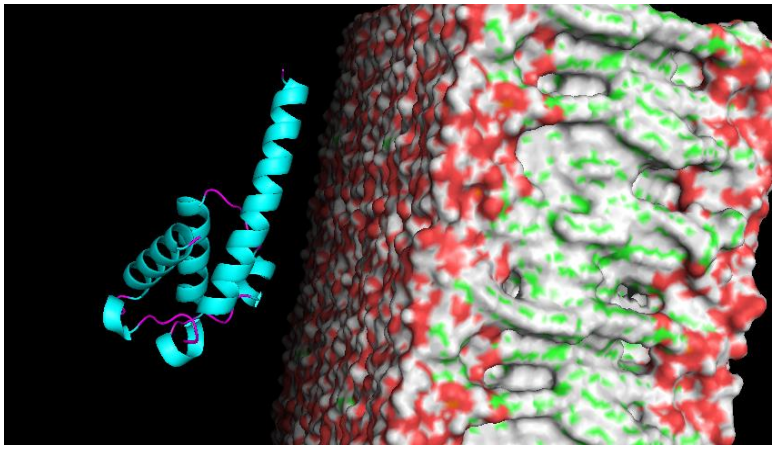

Figure 4. Bicelle crystalline solution is one method of inducing partial alignment.

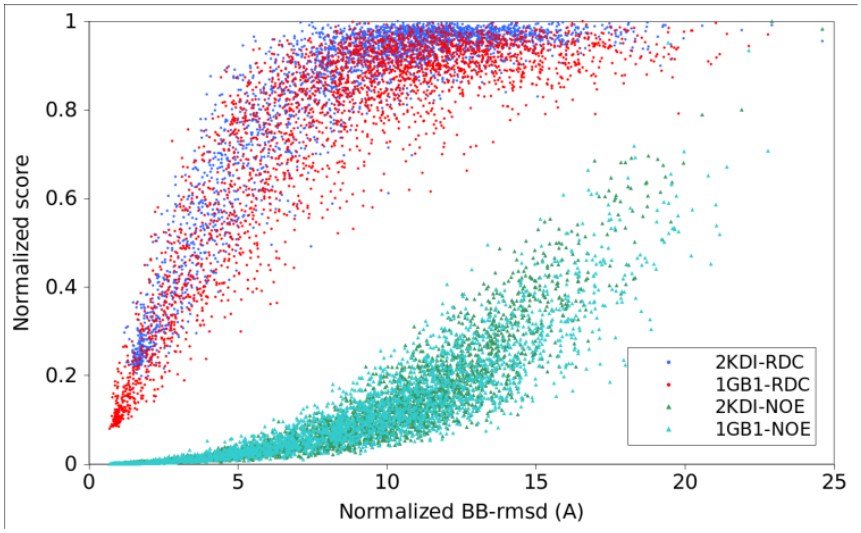

Figure 5. RDC and NOE fitness of 5000 decoy structures generated randomly from a known structure versus their backbone rmsd to the actual structure.

RDC data have several advantages over the conventional NOE data(8-14). In the interest of brevity, we focus our discussion on the importance of RDC data in high-resolution structure determination. Figure 5 represents the RDC and NOE fitness of 5000 derivative structures as a

function of their BB-RMSD to the known structure. These 5000 structures have been derived from a target protein by randomly altering the backbone torsion angles to achieve a continuum of distortions (measured in BB-RMSD's). Fitness to the experimental data (similar to Q-factor(31)) is calculated and plotted on the vertical axis, while BB-RMSD to the high-resolution structure is plotted on the horizontal axis. This figure illustrates the sensitivity of NOEs and RDCs as reporters of protein structures. Figure 5 suggests that NOEs tend to lose sensitivity as the search approaches the native structure, while RDCs become more sensitive. RDCs can also report molecular motions on timescales ranging from picoseconds to microseconds(62-64), during which many functionally important events occur. Indeed, in the 10 ns – 1 s timescale window, RDCs are the most sensitive of NMR parameters[32].

Despite many advantages of RDCs in characterization of protein structures, only a handful of protein structures submitted to the PDB have been determined exclusively by RDC data. Nearly all of the structures determined by RDCs have utilized an excessive number of RDCs than necessary(25-28) or resorted to the use of other experimental data such as NOEs, dihedral restraints and hydrogen bond restraints(21, 65, 66) for successful structure determination. Both of these approaches nullify the advantages of using RDCs (minimal data, reduced cost), and have therefore resulted in the failure to realize the full potential of RDCs.

REDCRAFT

Realization of the full potential of RDC data has been historically hindered by the lack of appropriate analysis tools. Practically, all of the legacy NMR data analysis software such as Xplor-NIH, CNS, or CYANA have been modified to incorporate RDC data into their analysis. However, the energy landscape that is created by the RDC data is far too complex to be navigated by

347 simplistic optimization routines such as Gradient Descent or Monte Carlo sampling. Therefore,
348 the legacy software can use RDC data only when they are accompanied by a large number of
349 traditional constraints. Structure determination based primarily on RDC data requires new
350 programs that operate in fundamentally different ways than those that use traditional constraints
351 such as NOE data.

352 In recent years, several computational approaches have been introduced with a focus on
353 structure determination of proteins from RDC data. REDCRAFT is such a program that sets itself
354 apart from other existing software packages in a number of ways. By deploying a novel search
355 mechanism that is significantly different than traditional optimization techniques, REDCRAFT
356 can accomplish the same outcome as other algorithms but with less data. REDCRAFT also
357 presents the ability for simultaneous study of structure and dynamics of proteins, and its
358 predecessor has demonstrated the capability for simultaneous structure elucidation and assignment
359 of data. Using simulated data, the success of REDCRAFT has been demonstrated with as little as
360 two RDCs per residue(34, 67, 68), or one RDC per residue(67, 69) when combined with backbone
361 torsion angle constraints. Meaningful structure determination, based on a subset of RDC data (two
362 or three per residue) obtained from the perdeuterated proteins, is critical in extending the structure
363 determination based on RDCs to large proteins. It is a common practice to deuterate the sample of
364 large proteins, leaving a far smaller selection of RDCs that can be collected. In particular, the set
365 of {C'-H, N-H, C'-N} RDC data can be obtained from deuterated proteins with relative ease. It
366 is therefore of great importance for any RDC-based structure determination technique to be able
367 to characterize structures from this subset of data. In this report we will demonstrate the success
368 of REDCRAFT in calculation of protein structures under these sparse data conditions.

369 REDCRAFT is also the only publicly available software package that is developed using a

370 sound Object Oriented (OO) programming paradigm, and it therefore lends itself well to
371 encapsulation of the physical and biophysical properties of proteins. For instance, the construction
372 of a Polypeptide object from the more fundamental Atom and AminoAcid objects, directly reflects
373 the natural process of polymerization and translates into better source code readability as well as
374 faster development and program execution. In addition, OO design allows for easier extendibility
375 of the system. For example, while the main data source of REDCRAFT is currently RDCs, one
376 could easily extend the architecture to use NOEs or RCSAs. The only changes that the developer
377 would need to make is the scoring mechanism of the elongation process and addition of any new
378 atoms needed for the new data source. Existence of the AminoAcid class makes the addition of
379 new atoms straightforward.

380 REDCRAFT's approach to structure determination proceeds in two stages denoted as
381 Stage-I and Stage-II. In Stage-I, a list of all possible torsion angles adjoining any two neighboring
382 peptide planes is pruned and ranked based on structural fitness to the RDC data. Pruning of the
383 local torsion angles can be based on scalar coupling data, maximum RDC fitness, dihedral
384 constraints (such as Ramachandran or TALOS), or on evolutionary relationship to other proteins
385 with an existing structure. Theoretically, the torsion angles adjoining any two peptide planes with
386 the best fitness to the RDC data should constitute the correct geometry and therefore structure
387 determination would be completed. Practically however, the globally optimal geometry will nearly
388 always not be ranked as the first (due to experimental or structural noise); necessitating a more
389 global search. Stage-II of REDCRAFT is designed to perform global optimization by elongating
390 (similar to the elongation process during protein synthesis) a given fragment of size N peptide
391 planes (initially a single dipeptide seed) by one peptide plane iteratively. Various conformers of
392 the new extended fragment are systematically generated and ranked based on fitness to the RDC

393 data (of the entire fragment). Typically, the top 2,000-10,000 structural candidates with the best
394 fitness to the RDC data are propagated for extension in the next round of elongation. This process
395 maintains a sufficiently diverse population of conformers to prevent entrapment in any one local
396 minimum and is the primary reason for the success of REDCRAFT in characterization of protein
397 structures with less data. The gradually increasing computational complexity of REDCRAFT is in
398 stark contrast to the traditional methods of folding the entire protein at once. By starting the
399 calculation for the entire protein, the algorithm must contend with the maximum level of
400 complexity from the start, which transforms the problem into a global optimization. This, by in
401 large, makes computation slower and limits the success due to inherent issues with high-
402 dimensional global optimization problems such as entrapment in local minima. In contrast,
403 REDCRAFT allows for structure calculation of a protein to proceed in an incrementally growing
404 fragment that provides a optimization with a gradually increasing complexity. By utilizing this
405 unique elongation approach, REDCRAFT is also capable of performing fragmented studies in
406 which only certain sections of the protein can be characterized. Fragmented studies are useful in
407 cases of missing or erroneous data. In the case of RDCs, which are very sensitive probes of internal
408 dynamics, REDCRAFT's fragmented study can be used to pinpoint the exact point of
409 dynamics(34, 41, 70). It is also worth noting that even though the REDCRAFT engine only
410 computes the backbone structure to reduce complexity, there are several methods available that
411 can accurately calculate the sidechains of a protein based solely on the backbone(71).

412 REDCRAFT also provides several filtering and constraining tools that are uniquely useful
413 for use with RDC data. For instance, Order Tensor Filter (OTF) allows selection of proteins based
414 on prior knowledge of order tensors(72, 73). REDCRAFT also allows the user to define dihedral
415 restraints. All restraints (including OTF and dihedral) can be flexibly turned on and off for select

416 regions of a protein that may suffer from severe lack of experimental data. The most recent version
417 of REDCRAFT (version 4.0) has also adopted NEF compliance in data import/export procedures,
418 and has incorporated an advanced decimation process that has allowed for successful structure
419 calculation of proteins with as much as ±4Hz of experimental noise(67, 69).

420 **Evaluation**

421 Our evaluation of REDCRAFT was conducted in three phases with increasing level of
422 difficulty in structure determination. In the first phase, REDCRAFT was tested using a set of
423 proteins with existing experimental RDCs and X-ray or NMR structures. In the second phase,
424 large proteins (larger than 500 residues) were chosen based on the availability of RDC data.
425 Although a few large proteins have been subjected to RDC data acquisition, none contained
426 enough RDC data to perform a meaningful structure calculation. In such instances, simulated
427 RDCs were generated for a sparse set of interacting vectors. REDCRAFT was then used to
428 calculate a RDC-based structure for each target protein to demonstrate the feasibility of RDC based
429 structure calculation of larger proteins. The rationale for this phase is to illustrate the possibility of
430 structure determination by RDCs when the collection of RDCs has been demonstrated in previous
431 work. In the last phase of the study, a novel protein was targeted for a simultaneous study by RDC
432 (using REDCRAFT) and NOE-based structure calculation. In each phase of the study structures
433 calculated by REDCRAFT are compared to the existing NMR and X-ray structures (if applicable)
434 of the respective proteins. The following sections provide more detailed information for each of
435 the proteins as well as an overview of the REDCRAFT algorithm.

436

437 **Target Proteins.**

438 During the first phase of our experiment, we selected the target proteins (shown in Table

439 4) based on the availability of RDC data in BMRB or PDB, structural diversity, and existence of
440 NMR or X-ray structure. RDC data for all the proteins except SR10 were obtained from the
441 BMRB(30), while the RDC data for SR10 were obtained from the SPINE database(35). More
442 detailed information regarding the exact RDCs can be found in the Table S1 of the Supplementary
443 Material. Table 4 provides some self-explanatory information for each protein including the final
444 column that highlights the average backbone similarity between the X-ray and NMR structures.

445 The protein GB1 has been previously studied in depth(28, 74) and represents an ideal
446 candidate to be used as a "proof of concept" case. GB3, an analog of GB1, was also investigated
447 in this study using a different set of RDCs. The RDCs for the GB3 were previously collected(32,
448 33) for refinement of a solved crystal structure to obtain better fitness to experimental data
449 (resulting in PDB ID 1P7E). Rubredoxin, represented another ideal target of study due to its mostly
450 coil structure. Traditionally, structures that are heavily composed of helical regions prove difficult
451 to solve for computational methods due to the near-parallel nature of their backbone N-H^N RDC
452 vectors. ChR145, represents a larger, mixed beta-sheet and alpha helix protein. In a previous study,
453 this protein was extracted from the Cytophaga hutchinsonii bacteria and characterized using
454 traditional NMR restraints (primarily NOEs). Of interest, ChR145's primary sequence is unique
455 in the PDB. This fact alone makes its structural characterization difficult for any method that has
456 a dependency on database lookups or homology modeling. SR10, a 145-residue protein, was
457 characterized as part of the Protein Structure Initiative(75) and was included in this study to
458 represent a challenging case because of the low RDC data density. The RDC data for this protein
459 consisted of only {N-H^N} vectors collected in three alignment media. Of additional interest, the
460 RDCs were collected on a perdeuterated version of the SR10 protein.

461

462 Table 4. List of protein targets with their respective X-ray and NMR reference structures,

RDCs used and the average BB-RMSD between the NMR and x-ray structures.

Target Name	NMR PDB ID	X-Ray PDB ID	# Res.	RDCs in M1/M2/M3	Avg. BB-RMSD
GB1	2PLP(28)	1IGD(76)	54	{C'-H, N-H^N, C'-N} / {N-H}	0.677Å
GB3	1P7E(77)	1IGD(76)	54	{C'-H, N-H^N} / {C'-H, N-H^N}	0.347Å
Rubredoxin	1RWD(10)	1IU5(78)	50	{C'-H, N-H^N} / {C'-H, N-H^N}	1.863Å
ChR145	2LEQ(35)	N/A	145	{N-H^N, C'-N} / {N-H^N, C'N} / {N-H^N}	NA
SR10	2KZN(79)	3E0O(80)	145	{N-H^N} / {N-H^N} / {N-H^N}	2.911

Currently there are very few examples of large proteins in the BMRB database that include RDC data. If RDC data are available for large proteins, they are very scarce and from only one alignment medium. Meaningful structure determination of proteins from RDC data requires RDC data in two alignment media(81). Therefore, to investigate the feasibility of protein structure calculation of large proteins using only RDCs, synthetic sets of {C'-H, N-H^N, C'-N}RDCs were generated in two alignment media using the software package REDCAT(61, 82) as described previously(83). A random error in the range of ±1 Hz was added to each vector to better simulate the experimental conditions. The proteins chosen for this controlled study are summarized in Table 5. Note that for ChR145 a synthetic study was also performed to demonstrate the unfragmented structure determination if additional RDC data had been acquired. It is noteworthy that Enzyme 1 from E. *coli* was chosen as an example of a large mixed α/β protein. The dataset used for solving the NMR structure of this protein included a very sparse set of {N-H^N} RDCs that was not applicable in our studies, but demonstrates the possibility of RDC data collection in large proteins.

Table 5. List of protein targets used in the synthetic study of large proteins.

Target Name	X-ray PDB ID	NMR PDB ID	# Res.	RDCs in M1/M2
ChR145	2LEQ(35)	N/A	145	{C'-H, N-H^N, C'-N}/ {C'-H, N-H^N, C'-N}

Lpg1496	5T8C	N/A	294	{C'-H, N-H^N, C'-N}/ {C'-H, N-H^N, C'-N}
Enzyme 1 from E. *coli*	N/A	2KX9(84)	573	{C'-H, N-H^N, C'-N}/ {C'-H, N-H^N, C'-N}

In addition to the previously characterized proteins, RDC data were acquired for a novel, 71-residue protein (designated PF2048.1). PF2048.1 has been selected as a target of our studies due to its novelty in comparison to the existing archive of structurally characterized proteins. PF2048.1, an all-helical 9.16 kDa protein, exhibited less than 12% sequence identity to any structurally characterized protein in PDB (as of January 2019). The previously reported computational models of this structure(72) concluded the helical nature of this protein and resulted in an ensemble of structures with as much as 10Å of backbone diversity(68, 72, 73).

RDC data were acquired by NMR spectroscopy for this protein in Phage and stretched Poly Acrylamide Gel (PAG) alignment media. The resulting two sets of RDCs consisted of {N-C', N-H^N, C'-H} from the Phage and {N-H^N} from the PAG media. The process of NMR data collection is described at length in Section 2.3. Collectively, the two data sets were missing ~17% of data points (48/276) leaving 228 total RDC data points (an average of 1.6 RDCs per residue, per alignment medium).

PF2048.1

Expression and Purification.

Expression and purification were performed by Nexomics Inc. Prior to gene synthesis, the sequence was optimized by codon optimization software. The designed gene was synthesized by Synbio-Tech (www.Synbio-tech.com) and subcloned into pET21-NESG vector.

Protein expression was performed as previously reported(85). Briefly, the recombinant pET21-NxSC1 plasmid was transformed into *E. coli* BL21 (DE3) cells and the cells were cultured

501 in $^{13}C^{15}N$-MJ9 medium containing 100 μg/mL of ampicillin. The culture was further incubated at
502 37°C and protein expression was induced by addition of isopropyl β-D-1-thiogalactopyranoside
503 (IPTG) to the final concentration of 1 mM at logarithmic phase. Cells were harvested after
504 overnight culture at 18°C and protein expression was evaluated by SDS-PAGE.

505 The protein was purified using a standard Ni affinity followed by size exclusion two-step
506 chromatography method first as previously reported(85). Since the purified NxSC1 sample
507 presented as 2 bands, an additional ion exchange chromatography was performed. The NxSC1
508 sample from the two-step purification was pooled and dialyzed against buffer A (Buffer A: 20 mM
509 Tris-HCl, pH 7.5), and loaded onto a HiTrap Q HP 5 ml column. A gradient of NaCl from 0 to 1
510 M was applied (Buffer B: 20 mM Tris-HCl, pH 7.5, 1 M NaCl). The NxSC1 was pooled and
511 concentrated to 1 mM using Amico Ultra-4 (Millipore).

512

513 **NMR Sample Preparation and Data Acquisition of PF2048.1**.

514 For measurements under isotropic conditions a sample of PF2048.1 was prepared at a
515 concentration of 0.8 mM in 20 mM MES, 100 mM NaCl, and 5 mM $CaCl_2$ at pH 6.5. All samples
516 also contained 10 mM DTT, 0.02% NaN_3, 1 mM DSS, and 10% D2O. An anisotropic sample is
517 required for the measurement of RDCs. After isotropic data collection, the PF2048.1 sample was
518 used to prepare two partially aligned samples. A sample with pf1 phage as the alignment medium
519 (designated alignment medium M1) was prepared which contained 0.88 mM PF2048.1 and 48
520 mg/mL phage in Tris buffer. After equilibration at room temperature for 10 min at 25 °C the sample
521 showed a deuterium splitting of 8.8 Hz when placed in the magnet. A second aligned sample was
522 prepared in a 5 mm Shigemi tube using positively charged poly-acrylamide compressed gels
523 (designated alignment medium M3). This sample contained approximately 0.77 mM PF2048.1.

524 After equilibration at 4 °C for 7–8 h the sample showed uniform swelling of the gel which is
525 compressed vertically.

526 NMR data were collected at 25ºC using Bruker Avance II 600 and 800 MHz spectrometers
527 equipped with 5-mm cryoprobes. Sequence specific backbone and side-chain NMR resonance
528 assignments were determined using standard triple-resonance NMR experiments (Table S2).
529 Processing of NMR spectra was done using TopSpin and NMRPipe whereas visualization was
530 done using NMRDraw and Sparky. NMR spectra were analyzed by consensus automated backbone
531 assignment analysis using PINE(86) and AutoAssign(87) software, and then extended by manual
532 analysis to determine resonance assignments. The solution NMR stricture was calculated using
533 CYANA using backbone and side-chain chemical shifts, ^{15}N and^{13}C-edited NOESY, and phi (ϕ)
534 *and psi* (ϕ) dihedral angle constraints derived from TALOS. Calculations using CYANA were
535 done iteratively to refine NOESY peak lists, verify and complete resonance assignments using
536 interactive spectral analysis with RPF(88) and Sparky(86) software. The 20 lowest energy
537 conformers of 100 calculated structure, based on target function scoe, were further refined by
538 simulated annealing and molecular dynamics in explicit water using CNS. Structure quality scores
539 were calculated using Protein Structure Validation Suite (PSVS)(89) and the goodness-of-fit
540 between the NOESY peak lists and the final ensemble of conformers were derived from RFP
541 software.

542

543 **Structure Calculation with NOEs**

544 Uniformly ^{13}C,^{15}N-enriched PF2048.1, a 72-residue protein, was used for NMR structure
545 determination, using standard triple-resonance NMR methods outlined in the Methods and
546 Materials. The structure was determined from ^{15}N- and ^{13}C-resolved 3D-NOESY data, both with

547 and without RDC restraints. In total 217 RDC measurements were used: 54 HC', 54 NC', 57 HN
548 RDC from medium 1 (M1 - phage), and 52 HN RDC from medium 2 (M3 –stretched
549 polyacrylamide gel). Both ASDP(90) and CYANA3.97(17) were used to automatically assign
550 long-range NOEs and to calculate these structures. ASDP(90) was also used to guide the iterative
551 cycles of noise/artifact NOESY peak removal, peak picking and NOE assignments, as described
552 elsewhere(91). NOE matching tolerances of 0.030, 0.03 and 0.40 ppm were used for indirect ^{1}H,
553 direct ^{1}H, and heavy atom ^{13}C/^{15}N dimensions, respectively, throughout the CYANA and ASDP
554 calculations. This analysis provided > 2,300 NOE-derived conformationally-restraining distance
555 restraints (Supplementary Tables S1 and S2). In addition, 132 backbone dihedral angle restraints
556 were derived from chemical shifts, using the program TALOS_N(92), together with 70-74
557 hydrogen-bond restraints. Structure calculations were then carried out using ~ 35 conformational
558 restraints per residue. One hundred random structures were generated and annealed using 10,000
559 steps. Similar results were obtained using both Cyana and ASDP automated analysis software
560 programs. The 20 conformers with the lowest target function value from the CYANA calculations
561 were then refined in an 'explicit water bath' using the program CNS and the PARAM19 force
562 field(93), using the final NOE derived distance restraints, TALOS_N dihedral angle restraints, and
563 hydrogen bond restraints derived from CYANA. Structure quality factors were assessed using the
564 PDBStat(88) and PSVS 1.5(89) software packages. The global goodness-of-fit of the final
565 structure ensemble with the NOESY peak list data were determined using the RPF analysis
566 program(88).

567 **Structure Calculation with REDCRAFT**

568 REDCRAFT(13, 34, 40, 41, 67, 68, 70, 94) was used to calculate the structure of proteins
569 from RDC data with a standard depth search of 1000. Additional features such as decimation(41),

570 minimization(34), and 4-bond LJ(34) terms were included in all calculations. Other features such
571 as Order Tensor Filter(34), and Dynamically Adaptive Decimation(69) were not used in this
572 exercise. For evaluation purposes, the RDC-RMSD reported by REDCRAFT was converted to Q-
573 factor to assess the final models' fitness to RDC data. The backbone-RMSD (BB-RMSD) of
574 REDCRAFT structures to existing structures were calculated using the *align* function of
575 PyMOL(95) without the exclusion of any atoms.

576 Under certain circumstances, structure determination by REDCRAFT is recommended to
577 be conducted in discrete fragments. One such instance is based on gap in the experimental data. In
578 comparison to the NOE-based structure determination, this can be a very powerful feature.
579 Fragmented study of a protein allows direct study of a certain region of interest in a protein and
580 therefore reduce the overall cost of data acquisition. A second instance relates to structure
581 determination of large proteins, during which accumulation of structural noise may influence the
582 course of structure determination. Departure from ideal peptide geometries (e.g. planarity of the
583 peptide plane), variation in bond distances, and bond angles can be cited as examples of structural
584 noise. The effect of structural noise, sometimes, accrues to become noticeable for fragments larger
585 than one hundred amino acids. Any existing gaps of less than 6 amino acids can easily be filled
586 during the process of structural refinement. In this study we have used XPLOR-NIH(15) to address
587 variation from ideal peptide geometries and complete the missing gaps. More specifically, during
588 the final refinement process, each structure was subjected to 30,000 steps of Powell minimization
589 that included the same set of RDCs used during the structure calculation with REDCRAFT. Aside
590 from completion of the missing residues, these minimizations normally resulted in structural
591 variation of less than 0.5A.

592 **Acknowledgements**

Funding for this project was provided by NIH grants P20 RR-016461 (to HV) and 1R01GM120574 (to GTM).

Conflict of Interest Statement

G.L. is an officer of Nexomics Bioscience, a contract research organization, G.T.M. is the founder of Nexomics Biosciences.

References

Supplementary Information

S1 Table. Structure Calculation Input Files

S2 Table. Structure Quality Statistics

S1 Figure. Solution NMR structure of PF2048.1 refined with RDC (green) and without RDC (cyan). The overall RMSD is within 0.6 Å.

REFERENCES

1. Berman HM, Battistuz T, Bhat TN, Bluhm WF, Bourne PE, Burkhardt K, et al. The Protein Data Bank. Acta Crystallogr D Biol Crystallogr. 2002;58(Pt 6 No 1):899-907.
2. Berman HM, Westbrook J, Feng Z, Gilliland G, Bhat TN, Weissig H, et al. The Protein Data Bank. Nucleic Acids Res. 2000;28:235-42.
3. Deshpande N, Addess KJ, Bluhm WF, Merino-Ott JC, Townsend-Merino W, Zhang Q, et al. The RCSB Protein Data Bank: a redesigned query system and relational database based on the mmCIF schema. Nucleic Acids Res. 2005;33(Database issue):D233-7.
4. Greshenfeld NA. The Nature of Mathematical Modeling. 1998.
5. Press WH, Teukolsky SA, Vettering WT, Flannery BP. Numerical Recipes in C++: The Art of Scientific Computing (2nd edn) 1 Numerical Recipes Example Book (C++) (2nd edn) 2 Numerical Recipes Multi-Language Code CD ROM with LINUX or UNIX Single-Screen License Revised Version 3. European Journal of Physics. 2003;24:329-30.
6. Wüthrich K, Billeter M, Braun W. Polypeptide secondary structure determination by nuclear magnetic resonance observation of short proton-proton distances. Journal of Molecular Biology. 1984;180:715-40.
7. Caflisch A, Niederer P, Anliker M. Monte Carlo minimization with thermalization for global optimization of polypeptide conformations in cartesian

632 coordinate space. Proteins. 1992;14(1):102-9.
633 8. de Alba E, Tjandra N. Residual dipolar couplings in protein structure
634 determination. Methods Mol Biol. 2004;278:89-106.
635 9. Chen K, Tjandra N. The use of residual dipolar coupling in studying
636 proteins by NMR. Topics in current chemistry. 2012;326:47-67.
637 10. Tian F, Valafar H, Prestegard JH. A dipolar coupling based strategy for
638 simultaneous resonance assignment and structure determination of protein
639 backbones. Journal of the American Chemical Society. 2001;123:11791-6.
640 11. Valafar H, Mayer K, Bougault C, LeBlond P, Jenney FE, Brereton PS, et al.
641 Backbone solution structures of proteins using residual dipolar couplings:
642 application to a novel structural genomics target. J Struct Funct Genomics.
643 2005;5:241-54.
644 12. Prestegard JH, Mayer KL, Valafar H, Benison GC. Determination of protein
645 backbone structures from residual dipolar couplings. Methods in enzymology.
646 2005;394:175-209.
647 13. Bryson M, Tian F, Prestegard JH, Valafar H. REDCRAFT: a tool for
648 simultaneous characterization of protein backbone structure and motion from RDC
649 data. Journal of Magnetic Resonance. 2008;191:322-34.
650 14. Prestegard JH, Valafar H, Glushka J, Tian F. Nuclear magnetic resonance
651 in the era of structural genomics. Biochemistry. 2001;40:8677-85.
652 15. Schwieters CD, Kuszewski JJ, Tjandra N, Clore GM. The Xplor-NIH NMR
653 molecular structure determination package. Journal of Magnetic Resonance.
654 2003;160:65-73.
655 16. Brunger AT, Adams PD, Clore GM, DeLano WL, Gros P, Grosse-Kunstleve RW,
656 et al. Crystallography & NMR system: A new software suite for macromolecular
657 structure determination. Acta crystallographica Section D, Biological
658 crystallography. 1998;54:905-21.
659 17. Güntert P. Automated NMR structure calculation with CYANA. Methods Mol
660 Biol. 2004;278:353-78.
661 18. Rohl CA, Baker D. De novo determination of protein backbone structure
662 from residual dipolar couplings using Rosetta. Journal of the American Chemical
663 Society. 2002;124:2723-9.
664 19. Ruan K, Briggman KB, Tolman JR. De novo determination of internuclear
665 vector orientations from residual dipolar couplings measured in three
666 independent alignment media. J Biomol NMR. 2008;41:61-76.
667 20. Blackledge M. Recent progress in the study of biomolecular structure and
668 dynamics in solution from residual dipolar couplings. Progress in Nuclear
669 Magnetic Resonance Spectroscopy. 2005;46:23-61.
670 21. Wang L, Donald BR. Exact solutions for internuclear vectors and backbone
671 dihedral angles from NH residual dipolar couplings in two media, and their
672 application in a systematic search algorithm for determining protein backbone

673 structure. Journal of biomolecular NMR. 2004;29:223-42.
674 22. Jung Y-SS, Sharma M, Zweckstetter M. Simultaneous assignment and structure
675 determination of protein backbones by using NMR dipolar couplings. Angewandte
676 Chemie (International Ed in English). 2004;43:3479-81.
677 23. Andrec M, Harano Y, Jacobson MP, Friesner RA, Levy RM. Complete protein
678 structure determination using backbone residual dipolar couplings and sidechain
679 rotamer prediction. Journal of structural and functional genomics. 2002;2:103-
680 11.
681 24. Delaglio F, Kontaxis G, Bax A. Protein Structure Determination Using
682 Molecular Fragment Replacement and NMR Dipolar Couplings. Journal of the
683 American Chemical Society. 2000;122:2142-3.
684 25. Hus J-C, Marion D, Blackledge M. Determination of protein backbone
685 structure using only residual dipolar couplings. Journal of the American
686 Chemical Society. 2001;123:1541-2.
687 26. Tolman JR. A novel approach to the retrieval of structural and dynamic
688 information from residual dipolar couplings using several oriented media in
689 biomolecular NMR spectroscopy. Journal of the American Chemical Society.
690 2002;124:12020-30.
691 27. Bouvignies G, Markwick P, Brüschweiler R, Blackledge M. Simultaneous
692 Determination of Protein Backbone Structure and Dynamics from Residual Dipolar
693 Couplings. Journal of the American Chemical Society. 2006;128:15100-1.
694 28. Bouvignies G, Meier S, Grzesiek S, Blackledge M. Ultrahigh-resolution
695 backbone structure of perdeuterated protein GB1 using residual dipolar couplings
696 from two alignment media. Angew Chem Int Ed Engl. 2006;45:8166-9.
697 29. Levenberg K. A method for the solution of certain problems in least
698 squares. Quarterly of Applied Mathematics. 1944;2:164 - 8.
699 30. Ulrich EL, Akutsu H, Doreleijers JF, Harano Y, Ioannidis YE, Lin J, et
700 al. BioMagResBank. Nucleic acids research. 2008;36:D402-8.
701 31. Cornilescu G, Marquardt JL, Ottiger M, Bax A. Validation of Protein
702 Structure from Anisotropic Carbonyl Chemical Shifts in a Dilute Liquid
703 Crystalline Phase. Journal of the American Chemical Society. 1998;120:6836-7.
704 32. Yao L, Vögeli B, Torchia DA, Bax A. Simultaneous NMR study of protein
705 structure and dynamics using conservative mutagenesis. J Phys Chem B.
706 2008;112:6045-56.
707 33. Clore GM, Schwieters CD. Amplitudes of protein backbone dynamics and
708 correlated motions in a small alpha/beta protein: correspondence of dipolar
709 coupling and heteronuclear relaxation measurements. Biochemistry.
710 2004;43:10678-91.
711 34. Simin M, Irausquin S, Cole CA, Valafar H. Improvements to REDCRAFT: a
712 software tool for simultaneous characterization of protein backbone structure
713 and dynamics from residual dipolar couplings. Journal of biomolecular NMR.

714 2014;60:241-64.
715 35. Prestegard J, Szyperski T, Montelione GT. SPiNE Data Base of RDC Data for
716 NESG Proteins. 2015.
717 36. Goodsell DS, Zardecki C, Di Costanzo L, Duarte JM, Hudson BP, Persikova
718 I, et al. RCSB Protein Data Bank: Enabling biomedical research and drug
719 discovery. Protein Sci. 2020;29(1):52-65.
720 37. Laskowski RA, MacArthur MW, Moss DS, Thornton JM. PROCHECK: a program to
721 check the stereochemical quality of protein structures. Journal of Applied
722 Crystallography. 1993;26:283-91.
723 38. Davis IW, Leaver-Fay A, Chen VB, Block JN, Kapral GJ, Wang X, et al.
724 MolProbity: all-atom contacts and structure validation for proteins and nucleic
725 acids. Nucleic Acids Res. 2007;35(Web Server issue):W375-83.
726 39. Huang YJ, Powers R, Montelione GT. Protein NMR recall, precision, and F-
727 measure scores (RPF scores): structure quality assessment measures based on
728 information retrieval statistics. Journal of the American Chemical Society.
729 2005;127:1665-74.
730 40. Shealy P, Simin M, Park SH, Opella SJ, Valafar H. Simultaneous structure
731 and dynamics of a membrane protein using REDCRAFT: membrane-bound form of Pf1
732 coat protein. Journal of Magnetic Resonance. 2010;207:8-16.
733 41. Valafar H, Simin M, Irausquin S. A Review of REDCRAFT. Annual Reports on
734 NMR Spectroscopy2012. p. 23-66.
735 42. Saupe A, Englert G. High-Resolution Nuclear Magnetic Resonance Spectra of
736 Orientated Molecules. Physical Review Letters. 1963;11:462-4.
737 43. Assfalg M, Bertini I, Turano P, Grant Mauk A, Winkler JR, Gray HB. 15N-
738 1H Residual dipolar coupling analysis of native and alkaline-K79A Saccharomyces
739 cerevisiae cytochrome c. Biophysical journal. 2003;84:3917-23.
740 44. Andrec M, Du PC, Levy RM. Protein backbone structure determination using
741 only residual dipolar couplings from one ordering medium. Journal of
742 biomolecular NMR. 2001;21:335-47.
743 45. Park SH, Marassi FM, Black D, Opella SJ. Structure and Dynamics of the
744 Membrane-Bound Form of Pf1 Coat Protein: Implications of Structural
745 Rearrangement for Virus Assembly. Biophysical Journal. 2010;99:1465-74.
746 46. Park SH, Son WS, Mukhopadhyay R, Valafar H, Opella SJ. Phage-induced
747 alignment of membrane proteins enables the measurement and structural analysis
748 of residual dipolar couplings with dipolar waves and lambda-maps. Journal of
749 the American Chemical Society. 2009;131:14140-1.
750 47. Cierpicki T, Liang BY, Tamm LK, Bushweller JH. Increasing the accuracy of
751 solution NMR structures of membrane proteins by application of residual dipolar
752 couplings. High-resolution structure of outer membrane protein A. J Am Chem
753 Soc. 2006.
754 48. Sass HJ, Musco G, Stahl SJ, Wingfield PT, Grzesiek S. Solution NMR of

755 proteins within polyacrylamide gels: diffusional properties and residual
756 alignment by mechanical stress or embedding of oriented purple membranes. J
757 Biomol NMR. 2000;18:303-9.
758 49. Im W, Brooks CLr. De novo folding of membrane proteins: an exploration of
759 the structure and NMR properties of the fd coat protein. J Mol Biol.
760 2004;337:513-9.
761 50. Cole CA, Mukhopadhyay R, Omar H, Hennig M, Valafar H. Structure
762 Calculation and Reconstruction of Discrete-State Dynamics from Residual Dipolar
763 Couplings. Journal of chemical theory and computation. 2016;12:1408-22.
764 51. Montalvao RW, Simone AD, Vendruscolo M. Determination of structural
765 fluctuations of proteins from structure-based calculations of residual dipolar
766 couplings. J Biomol NMR. 2012;53:281-92.
767 52. Bouvignies G, Markwick PRL, Blackledge M. Simultaneous definition of high
768 resolution protein structure and backbone conformational dynamics using NMR
769 residual dipolar couplings. Chemphyschem : a European journal of chemical
770 physics and physical chemistry. 2007;8:1901-9.
771 53. Lee S, Mesleh MF, Opella SJ. Structure and dynamics of a membrane protein
772 in micelles from three solution NMR experiments. J Biomol NMR. 2003;26:327-34.
773 54. Prestegard JH, Al-Hashimi HM, Tolman JR. NMR structures of biomolecules
774 using field oriented media and residual dipolar couplings. Quarterly reviews of
775 biophysics. 2000;33:371-424.
776 55. Bax A, Kontaxis G, Tjandra N. Dipolar couplings in macromolecular
777 structure determination. Methods in enzymology. 2001;339:127-74.
778 56. Tjandra N, Grzesiek S, Bax A. Magnetic Field Dependence of Nitrogen-Proton
779 J Splittings in 15 N-Enriched Human Ubiquitin Resulting from Relaxation
780 Interference and Residual Dipolar Coupling. Journal of the American Chemical
781 Society. 1996;118:6264-72.
782 57. Tolman JR, Flanagan JM, Kennedy MA, Prestegard JH, Tolman Flanagan JM,
783 Kennedy, M A & Prestegard, JH, J R. Nuclear Magnetic Dipole Interactions in
784 Field-Oriented Proteins - Information for Structure Determination in Solution.
785 Proc Natl Acad Sci U S A. 1995;92:9279-83.
786 58. Prestegard JH, Kishore AI. Partial alignment of biomolecules: an aid to
787 NMR characterization. Current opinion in chemical biology. 2001;5:584-90.
788 59. Nitz M, Sherawat M, Franz KJ, Peisach E, Allen KN, Imperiali B. Structural
789 origin of the high affinity of a chemically evolved lanthanide-binding peptide.
790 Angewandte Chemie (International ed in English). 2004;43:3682-5.
791 60. Bax A, Tjandra N. High-resolution heteronuclear NMR of human ubiquitin in
792 an aqueous liquid crystalline medium. Journal of biomolecular NMR. 1997;10:289-
793 92.
794 61. Valafar H, Prestegard JH. REDCAT: a residual dipolar coupling analysis
795 tool. Journal of magnetic resonance (San Diego, Calif : 1997). 2004;167:228-41.

62. Peti W, Meiler J, Bruschweiler R, Griesinger C. Model-free analysis of protein backbone motion from residual dipolar couplings. J Am Chem Soc. 2002;124:5822-33.
63. Meiler J, Prompers JJ, Peti W, Griesinger C, Brüschweiler R, Bruschweiler R. Model-free approach to the dynamic interpretation of residual dipolar couplings in globular proteins. Journal of the American Chemical Society. 2001;123:6098-107.
64. Tolman JR, Flanagan JM, Kennedy MA, Prestegard JH. NMR evidence for slow collective motions in cyanometmyoglobin. Nat Struct Biol. 1997;4:292-7.
65. Yershova A, Tripathy C, Zhou P, Donald BR. Algorithms and Analytic Solutions Using Sparse Residual Dipolar Couplings for High-Resolution Automated Protein Backbone Structure Determination by NMR. 2010. p. 355-72.
66. Zeng J, Boyles J, Tripathy C, Wang L, Yan A, Zhou P, et al. High-resolution protein structure determination starting with a global fold calculated from exact solutions to the RDC equations. Journal of biomolecular NMR. 2009;45:265-81.
67. Cole CA, Parks C, Rachele J, Valafar H. Improvements of the REDCRAFT Software Package. Proceedings of the International Conference on Bioinformatics and Computational Biology; Las Vegas, NV: The Steering Committee of The World Congress in Computer Science, Computer Engineering and Applied Computing (WorldComp); 2019. p. 54-60.
68. Cole CA, Ishimaru D, Hennig M, Valafar H. An Investigation of Minimum Data Requirement for Successful Structure Determination of Pf2048.1 with REDCRAFT: The Steering Committee of The World Congress in Computer Science, Computer Engineering and Applied Computing (WorldComp); 2015.
69. Cole CA, Parks C, Rachele J, Valafar H. Increased Usability, Algorithmic Improvements and Incorporation of Data Mining for Structure Calculation of Proteins with REDCRAFT Software Package. BMC Bioinformatics. 2020.
70. Hanin Omar CAC, Mirko Hennig, Homayoun Valafar. Characterization of discrete state dynamics from residual dipolar couplings using REDCRAFT. Columbia, SC USA2016.
71. Krivov GG, Shapovalov MV, Dunbrack RLJ. Improved prediction of protein side-chain conformations with SCWRL4. Proteins. 2009;77:778-95.
72. Fahim A, Mukhopadhyay R, Yandle R, Prestegard JH, Valafar H. Protein Structure Validation and Identification from Unassigned Residual Dipolar Coupling Data Using 2D-PDPA. Molecules (Basel, Switzerland). 2013;18:10162-88.
73. Bansal S, Miao X, Adams MWW, Prestegard JH, Valafar H. Rapid classification of protein structure models using unassigned backbone RDCs and probability density profile analysis (PDPA). Journal of Magnetic Resonance. 2008;192:60-8.
74. Lamley JM, Lougher MJ, Sass HJ, Rogowski M, Grzesiek S, Lewandowski JR.

Unraveling the complexity of protein backbone dynamics with combined 13 C and 15 N solid-state NMR relaxation measurements. Phys Chem Chem Phys. 2015;17:21997-2008.
75. Montelione GT. The Protein Structure Initiative: achievements and visions for the future. F1000 biology reports. 2012;4:7.
76. Derrick JP, Wigley DB. The third IgG-binding domain from streptococcal protein G. An analysis by X-ray crystallography of the structure alone and in a complex with Fab. J Mol Biol. 1994;243(5):906-18.
77. Ulmer TS, Ramirez BE, Delaglio F, Bax A. Evaluation of backbone proton positions and dynamics in a small protein by liquid crystal NMR spectroscopy. J Am Chem Soc. 2003;125:9179-91.
78. Chatake T, Kurihara K, Tanaka I, Tsyba I, Bau R, Jenney FE, Jr., et al. A neutron crystallographic analysis of a rubredoxin mutant at 1.6 A resolution. Acta Crystallogr D Biol Crystallogr. 2004;60(Pt 8):1364-73.
79. Lange OF, Rossi P, Sgourakis NG, Song Y, Lee H-W, Aramini JM, et al. Determination of solution structures of proteins up to 40 kDa using CS-Rosetta with sparse NMR data from deuterated samples. Proceedings of the National Academy of Sciences. 2012;109:10873-8.
80. Kim YK, Shin YJ, Lee WH, Kim HY, Hwang KY. Structural and kinetic analysis of an MsrA-MsrB fusion protein from Streptococcus pneumoniae. Mol Microbiol. 2009;72(3):699-709.
81. Al-Hashimi HM, Valafar H, Terrell M, Zartler ER, Eidsness MK, Prestegard JH. Variation of molecular alignment as a means of resolving orientational ambiguities in protein structures from dipolar couplings. Journal of magnetic resonance (San Diego, Calif : 1997). 2000;143:402-6.
82. REDCAT - Residual Dipolar Coupling Analysis Software Tool, (2003).
83. Schmidt C, Irausquin SJ, Valafar H. Advances in the REDCAT software package. BMC bioinformatics. 2013;14:302.
84. Schwieters CD, Suh JY, Grishaev A, Ghirlando R, Takayama Y, Clore GM. Solution structure of the 128 kDa enzyme I dimer from Escherichia coli and its 146 kDa complex with HPr using residual dipolar couplings and small- and wide-angle X-ray scattering. J Am Chem Soc. 2010;132(37):13026-45.
85. Xiao R, Anderson S, Aramini J, Belote R, Buchwald WA, Ciccosanti C, et al. The high-throughput protein sample production platform of the Northeast Structural Genomics Consortium. Journal of structural biology. 2010;172:21-33.
86. Lee W, Westler WM, Bahrami A, Eghbalnia HR, Markley JL. PINE-SPARKY: graphical interface for evaluating automated probabilistic peak assignments in protein NMR spectroscopy. Bioinformatics (Oxford, England). 2009;25:2085-7.
87. Zimmerman DE, Kulikowski CA, Huang YP, Feng WQ, Tashiro M, Shimotakahara S, et al. Automated analysis of protein NMR assignments using methods from artificial intelligence. 1997;269:592-610.

88. Tejero R, Snyder D, Mao B, Aramini JM, Montelione GT. PDBStat: a universal restraint converter and restraint analysis software package for protein NMR. J Biomol NMR. 2013;56(4):337-51.
89. Bhattacharya A, Tejero R, Montelione GT. Evaluating protein structures determined by structural genomics consortia. Proteins. 2007;66(4):778-95.
90. Huang YJ, Mao B, Xu F, Montelione GT. Guiding automated NMR structure determination using a global optimization metric, the NMR DP score. J Biomol NMR. 2015;62(4):439-51.
91. Huang YJ, Tejero R, Powers R, Montelione GT. A topology-constrained distance network algorithm for protein structure determination from NOESY data. Proteins: Structure, Function, and Bioinformatics. 2005;62:587-603.
92. Shen Y, Bax A. Protein structural information derived from NMR chemical shift with the neural network program TALOS-N. Methods in molecular biology (Clifton, NJ). 2015;1260:17-32.
93. Brooks BR, Bruccoleri RE, Olafson BD, States DJ, Swaminathan S, Karplus M. CHARMM: A program for macromolecular energy, minimization, and dynamics calculations. Journal of Computational Chemistry. 1983;4:187-217.
94. Timko E, Shealy P, Bryson M, Valafar H. Minimum Data Requirements and Supplemental Angle Constraints for Protein Structure Prediction with REDCRAFT2008.
95. DeLano WL. The PyMOL Molecular Graphics System. DeLano Scientific LLC, Palo Alto, CA, USA http://wwwpymolorg. 2008.